Monte Carlo Simulation of Electron Transport in the III-Nitride Wurtzite Phase Materials System: Binaries and Ternaries

Maziar Farahmand, *Member, IEEE*, Carlo Garetto, Enrico Bellotti, Kevin F. Brennan, *Senior Member, IEEE*, Michele Goano, *Member, IEEE*, Enrico Ghillino, Giovanni Ghione, *Senior Member, IEEE*, John D. Albrecht, and P. Paul Ruden, *Senior Member, IEEE*

***Abstract*—We present a comprehensive study of the transport dynamics of electrons in the ternary compounds, $Al_xGa_{1-x}N$ and $In_xGa_{1-x}N$. Calculations are made using a nonparabolic effective mass energy band model, Monte Carlo simulation that includes all of the major scattering mechanisms. The band parameters used in the simulation are extracted from optimized pseudopotential band calculations to ensure excellent agreement with experimental information and *ab initio* band models. The effects of alloy scattering on the electron transport physics are examined. The steady-state velocity field curves and low field mobilities are calculated for representative compositions of these alloys at different temperatures and ionized impurity concentrations. A field dependent mobility model is provided for both ternary compounds AlGaN and InGaN. The parameters for the low and high field mobility models for these ternary compounds are extracted and presented. The mobility models can be employed in simulations of devices that incorporate the ternary III-nitrides.**

***Index Terms*—Monte Carlo method, semiconductor materials, wide bandgap semiconductors.**

I. Introduction

THE WIDE bandgap semiconductor materials, particularly the III-nitrides, are of emerging importance in many semiconductor device applications. The III-nitride materials system includes the binary compounds, InN, GaN, and AlN and their associated ternaries, $In_xGa_{1-x}N$, $Al_xGa_{1-x}N$, and $In_xAl_{1-x}N$. The large direct energy gap of these materials makes them highly attractive for both optoelectronic and electronic devices [1]–[7]. The large band gap energy of the III-nitrides insures that the breakdown electric field strength of these materials is much larger than that of either Si or GaAs [8], [9], enabling, at least in principle, much higher maximum output power delivery in power amplifiers. Additionally, it has been found that at least the binary compounds, GaN and InN, have higher electron saturation drift velocities and lower dielectric constants that can lead to higher frequency performance of devices made from these materials [10].

The fact that GaN, InN and AlN, can form Type I heterojunctions with their related ternaries provides an additional advantageous quality for device design. Type I heterojunctions enable modulation doping techniques and their exploitation in MODFET devices. In addition, the lattice mismatch between GaN and the ternary compound AlGaN in appropriately designed structures produces strain induced polarization fields [11], [12]. These strain induced polarization fields can alter the band bending and carrier concentration at the heterointerface. In this way, the free carrier concentration can be increased within the channel region of a heterojunction field effect transistor, HFET, beyond that achievable by modulation doping alone [13]. The strain induced polarization fields can be further exploited to enhance the base conductivity in HBTs [14], and to alter the local impact ionization rates in a multiquantum well structure [15].

For the above stated reasons, the III-nitride materials are of great interest for power FET and optoelectronic device structures. To clarify the expected performance of these materials, transport as well as device studies are critical. Though there has been recent theoretical [16]–[27] and experimental [28]–[32] work on the transport properties of the binary compounds and their related devices [33]–[35], there has been little information about the transport properties of the ternary compounds [36]. It is the purpose of this paper to provide a comprehensive Monte-Carlo-based study of the key, low field, transport parameters of the III-nitride ternary compounds useful in device level simulation. Specifically, we present Monte-Carlo-based calculations of the electronic mobility and steady-state velocity field curves for various compositions of the InGaN and AlGaN ternary compounds. Using the parameters evaluated herein, simulation of devices that include the III-nitride ternary compounds can now proceed.

Manuscript received April 1, 2000; revised October 30, 2000. The work at Georgia Tech was sponsored in part by the Office of Naval Research through Contract E21-K19, through Subcontract E21-K69 made to Georgia Tech from the Office of Naval Research MURI Program at UCSB, the National Science Foundation through Grant ECS-9811366, by the National Phosphor Center of Excellence through Contract E21-Z22, and by the Yamacraw Initiative. The work at the University of Minnesota was supported by the National Science Foundation through Grant ECS-9811366, by the Office of Naval Research and by the Minnesota Supercomputer Institute. The work at Politecnico di Torino was partially supported by CNR (National Research Council) through the MADESS II Project. The review of this paper was arranged by Editor U. Mishra.

M. Farahmand is with Movaz Networks, Norcross, GA USA.

E. Bellotti and K. F. Brennan are with the School of Electrical and Computer Engineering, Georgia Tech, Atlanta, GA 30332-0250 USA (e-mail: fm@ieee.org).

C. Garetto, M. Goano, E. Ghillino, and G. Ghione are with the Dipartimento di Elettronica, Politecnico di Torino, Torino, Italy.

J. D. Albrecht and P. P. Ruden are with the Department of Electrical and Computer Engineering, University of Minnesota, Minneapolis, MN 55455 USA.

Publisher Item Identifier S 0018-9383(01)01465-4.

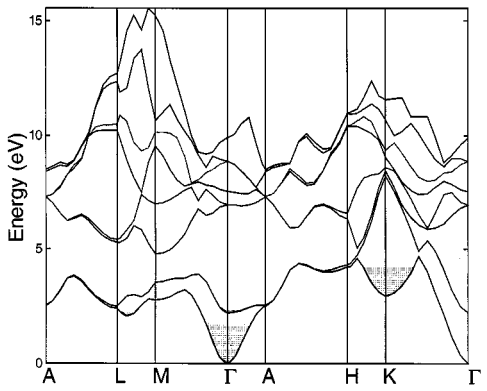

Fig. 1. Lowest eight conduction bands of wurtzite-phase GaN calculated by the empirical pseudopotential method. The shaded regions show the four lowest valleys.

II. Electronic Structure, Scattering Models and Other Parameters

Electronic transport is studied using the ensemble Monte Carlo simulation. The band structures of the materials under study are approximated with an analytical formulation using nonparabolic spherical valleys. Though usage of an analytical band structure is questionable at high-applied electric field strengths wherein impact ionization can occur, we adopt its usage here for the following reasons. First, due to the large number of compositions examined, it is too computationally expensive to utilize full band models with their concomitant numerically derived scattering mechanisms. Second, we have found that the analytical model well reflects the low field dynamics critical for assessing the carrier mobility. Since we restrict our work here only to low field phenomena, an analytical band structure is satisfactory. For each material four nonequivalent valleys have been included, as shown in Fig. 1. The primary valley for all materials occurs at Γ_1^c. The secondary minima included in the simulation are located at U, K, and Γ_3^c. It should be noted that their relative energy ordering varies among the materials studied. The U minima are located between the M and L symmetry points, and consist of six equivalent valleys. The K minima consist of two equivalent valleys. The electron energy dependence as a function of wave-vector in each valley is approximated using a first order nonparabolic relation. The band structure data used in these calculations have been determined from a novel adaptation of the pseudopotential method. For each constitutive atom in the compounds, the effective potentials are optimized using an iterative scheme in which the band structures are recursively calculated and selected features are compared to experimental and/or ab initio results. Using this technique, we have obtained an updated, highly accurate description of the band structures of the binary compounds. The band structures of the ternary compounds are determined from the binaries using the virtual crystal approximation. The nonparabolicity factors, effective masses and intervalley energy separations for the binary compounds, AlN, GaN, and InN wurtzite phase materials have been reported in [37]. The same parameters have been reported in [38] for the ternary compounds, $Al_xGa_{1-x}N$, $In_xGa_{1-x}N$, and $In_xAl_{1-x}N$.

The scattering mechanisms included within the simulation are: acoustic phonon scattering, nonpolar optical phonon (equivalent and nonequivalent intervalley) scattering, polar optical phonon scattering, ionized impurity scattering, piezoelectric scattering, and alloy scattering [39]. The scattering parameters for the binaries are taken from [40]–[47]. The scattering parameters for the ternary alloys are determined using linear interpolation. The parameters used in the calculations are reported in Table I for convenience. In the case of alloy scattering, the scattering rate is given as

$$W_{all}(E) = \frac{3\pi^3}{8\hbar} V_0 U_{Alloy}^2 x(1-x) N(E) \tag{1}$$

where

V_0 volume of the primitive cell of the direct lattice;
U_{Alloy} random alloy potential;
x alloy mole fraction;
$N(E)$ density of states.

Different interpretations for the choice of the random alloy potential have been given in the past. Littlejohn *et al.* [48] have used the conduction band offset (equal to the difference in the affinities) to represent the random scattering potential. Chin *et al.* [49] have determined the random potential from band gap bowing parameters and applying Phillips' theory of electronegativity differences [50]. In accordance with our previous work [51], we have made two sets of simulations to bracket the effect of alloy scattering. One set of simulations has been made using the alloy scattering potential calculated from whichever method that produces the highest value, to account for the worst case, i.e., strongest alloy scattering. In the other set of simulations the random alloy potential has been set to zero in order to account for the best case, i.e., no alloy scattering. The conduction band offsets have been calculated from the difference of the energy gaps using the known valence band offsets [52]. It was observed that calculation of the random potential from the conduction band offsets results in higher potentials than those calculated from the electronegativity differences. Therefore, the conduction band offsets were used to represent the random alloy potential in the first set of simulations.

III. Calculated Results

The steady-state electron drift velocity versus electric field has been calculated for the nitride binaries and ternaries at different temperatures and various doping concentrations. However, due to space limitations, we include results only for an ambient temperature of 300 K and an electron concentration of 10^{17} cm^{-3}. The low field mobility has been included at different temperatures and electron densities. In all cases the results for $In_xAl_{1-x}N$ have been excluded for brevity in favor of the more important $Al_xGa_{1-x}N$, and $In_xGa_{1-x}N$ materials.

Fig. 2 shows the calculated electron steady-state drift velocity versus applied electric field, for GaN, $Al_{0.2}Ga_{0.8}N$, $Al_{0.5}Ga_{0.5}N$, $Al_{0.8}Ga_{0.2}N$, and AlN materials. This set of calculations is made assuming the maximum alloy scattering rate. In this way, we can bracket the effect of alloy scattering by

TABLE I
MATERIAL PARAMETERS USED IN OUR MONTE CARLO CALCULATION. $\hbar\omega_{LO}$—POLAR OPTICAL PHONON ENERGY, ε_r, ε_{oo}—STATIC AND HIGH FREQUENCY RELATIVE PERMITIVITIES, D_a—DEFORMATION POTENTIAL, ρ_m—MASS DENSITY, v_s—SOUND VELOCITY, P_z—PIEZOELECTRIC CONSTANT, D_{ij}—INTERVALLEY DEFORMATION POTENTIAL, AND $\hbar\omega_{ij}$—NONPOLAR OPTICAL (INTERVALLEY) PHONON ENERGY. (a) CALCULATED BY AVERAGING OVER ALL PHONON ANGLES; (b) ASSUMED TO BE THE SAME AS GaAs

Parameter	GaN	InN	AlN
$\hbar\omega_{LO}$ (meV)	90.8811 [Ref. 40]	72.6553[Ref. 41]	110.3468 [Ref.42]
ε_r	9.7 [Ref. 43]	13.52 [Ref. 41]	8.5 [Ref. 45]
ε_∞	5.28 [Ref. 43]	8.4 [Ref. 41]	4.46 [Ref. 44]
D_a (eV)	8.3 [Ref. 45]	7.1 [Ref. 45]	9.5[Ref. 45]
ρ_m (kg/m^3)	6087 [Ref. 40]	6810 [Ref. 45]	3230[Ref. 45]
v_s (cm/s)	7619[a] [Ref. 40]	6238 [Ref. 45]	10910[a] [Ref. 46]
P_z (C/m^2)	0.375 [Ref. 45]	0.375 [Ref. 45]	0.92 [Ref. 47]
D_{ij} (10^9 eV/cm)	1[b]	1[b]	1[b]
$\hbar\omega_{ij}$ (meV)	65.8361 [Ref. 40]	55.4214 [Ref. 41]	75.7549 [Ref. 42]

[a] Calculated by averaging over all phonon angles.
[b] Assumed to be the same as GaAs

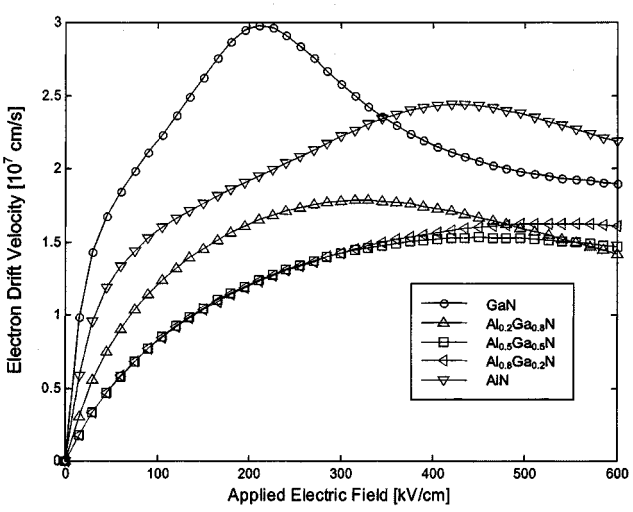

Fig. 2. Calculated electron drift velocity versus applied electric field for GaN, $Al_{0.2}Ga_{0.8}N$, $Al_{0.5}Ga_{0.5}N$, $Al_{0.8}Ga_{0.2}N$, and AlN. For this calculation, the random alloy potential was set equal to conduction band offsets. Lattice temperature is at 300 K, and electron concentration is equal to 10^{17} cm^{-3}.

comparing the calculations to the case where alloy scattering is omitted. The results of the calculation with no alloy scattering are shown in Fig. 3. It is interesting to compare the results of Figs. 2 and 3. The most striking difference is the effect of alloy scattering. It is observed that alloy scattering becomes the dominant scattering mechanism in these materials under the present simulation conditions, when the random alloy potential is set to the conduction band offset between GaN and AlN. A significantly lower drift velocity is observed when alloy scattering is present which is simply a result of the higher total scattering rate. Moreover, in the presence of alloy scattering the peak velocity occurs at a higher applied field compared to the case when alloy scattering is neglected. This is also due to the fact that in the presence of alloy scattering, the total scattering rate is higher; thus a higher field is required to heat the carriers prior to the onset of intervalley transfer.

It should be mentioned that the calculated drift velocities for GaN and AlN, as shown in Fig. 2, are slightly different than what we have previously reported [18], [19]. These differences are mainly due to the updated band structure parameters used in this study. Additionally, we have included piezoelectric scattering, which had been assumed to be negligible in some of the earlier calculations [19]. It should also be mentioned that if the bowing parameters are small, the Phillip's theory of electronegativity differences is consistent with a very small alloy scattering potential [49]. Our recent calculations [38] indicate that the bowing parameters may indeed be small. Under these conditions, the alloy scattering becomes negligible and the electron drift velocity as a function of the applied field approaches those shown in Fig. 3.

Fig. 4 shows the calculated electron drift velocity versus applied electric field for the GaN, In_2Ga_8N, In_5Ga_5N, In_8Ga_2N, and InN materials. The random alloy potential is set equal to the conduction band offsets. Similar to the case of the $Al_xGa_{1-x}N$ system, a second set of simulations, with zero alloy scattering is made in order to bracket the effect of alloy scattering. The

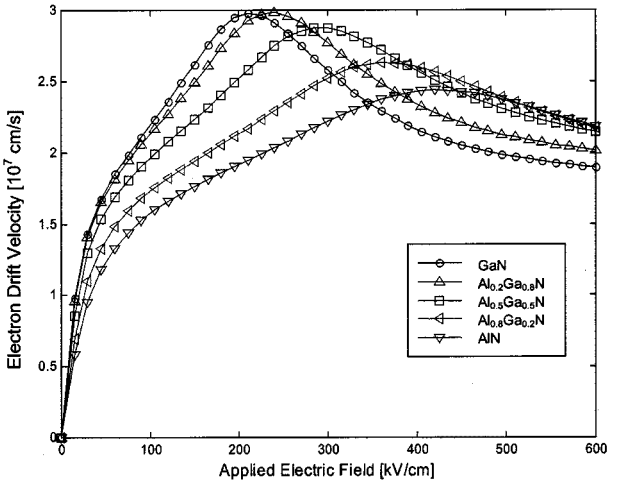

Fig. 3. Calculated electron drift velocity versus applied electric field for GaN, $Al_{0.2}Ga_{0.8}N$, $Al_{0.5}Ga_{0.5}N$, $Al_{0.8}Ga_{0.2}N$, and AlN. For this calculation, the random alloy potential was set to zero. Lattice temperature is at 300 K, and electron concentration is equal to 10^{17} cm^{-3}.

results of the latter calculation for the electron drift velocity are shown in Fig. 5. Similar comparisons and arguments applied to the case of Fig. 2 versus Fig. 3 also apply here. However it should be mentioned that for the $In_xGa_{1-x}N$ compound that the random alloy scattering potential calculated from Phillips' theory of electronegativity differences results in values on the same order as the conduction band offsets. Therefore if these values are used to calculate the alloy scattering, the results would be closer to that shown in Fig. 4.

It might be thought that since the electron peak velocity of InN is higher than that of GaN, it should also be higher than that of $In_{0.8}Ga_{0.2}N$. However, Fig. 5 shows a higher peak velocity in $In_{0.8}Ga_{0.2}N$ and $In_{0.5}Ga_{0.5}N$, than that of InN. This arises from

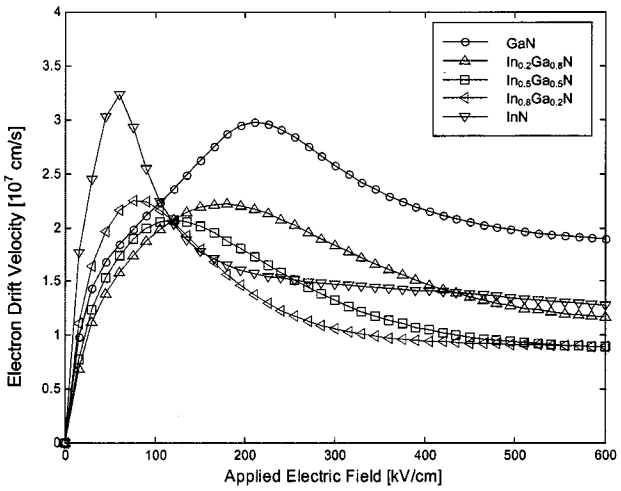

Fig. 4. Calculated electron drift velocity versus applied electric field for GaN, $In_{0.2}Ga_{0.8}N$, $In_{0.5}Ga_{0.5}N$, $In_{0.8}Ga_{0.2}N$, and InN. For this calculation, the random alloy potential was set equal to conduction band offsets. Lattice temperature is at 300 K, and electron concentration is equal to 10^{17} cm^{-3}.

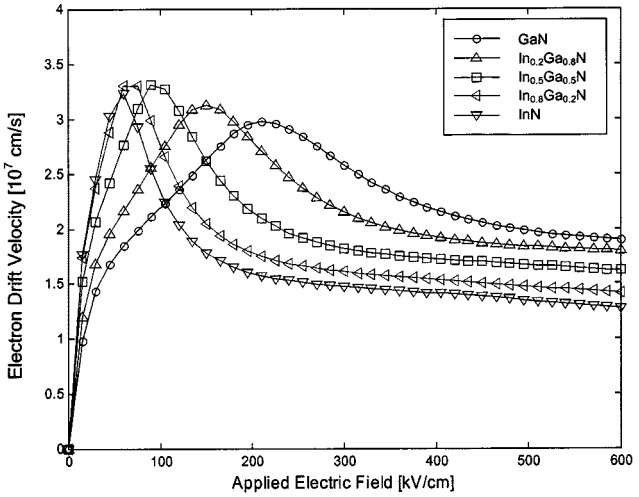

Fig. 5. Calculated electron drift velocity versus applied electric field for GaN, $In_{0.2}Ga_{0.8}N$, $In_{0.5}Ga_{0.5}N$, $In_{0.8}Ga_{0.2}N$, and InN. For this calculation, the random alloy potential was set to zero. Lattice temperature is at 300 K, and electron concentration is equal to 10^{17} cm^{-3}.

the fact that the peak velocity depends nonlinearly on the electron mobility in the lowest valley and the energy separation between this valley and the secondary valleys. By changing the In mole fraction in $In_xGa_{1-x}N$ from 1 to 0, the mobility decreases from that of InN to that of GaN, however the energy separation between the lowest valley and secondary valleys increases. Due to the nonlinear dependence of the peak velocity on these two factors, an initial increase followed by a decrease in the peak velocity with increasing Ga composition is observed, as shown in Fig. 5.

The low field electron mobility is also calculated for the binary compounds, and the ternaries, $Al_xGa_{1-x}N$ and $In_xGa_{1-x}N$ ($x = 0.2$, 0.5, 0.8). For $Al_xGa_{1-x}N$ and $In_xGa_{1-x}N$ the mobility is calculated for the two bracketing

TABLE II
CALCULATED LOW FIELD MOBILITY FOR LATTICE TEMPERATURE OF 300 K, AND A SET OF IONIZED IMPURITY CONCENTRATIONS OF 10^{16} cm^{-3}, 10^{17} cm^{-3}, AND 10^{18} cm^{-3}. U_{alloy} STANDS FOR THE RANDOM ALLOY POTENTIAL. ΔE_c IS THE BAND GAP OFFSET. FOR $Al_xGa_{1-x}N$, AND $In_xGa_{1-x}N$ MOBILITY HAS BBEEN CALCULATED FOR THE TWO BRACKETING CONDITIONS OF $U_{alloy} = 0$, AND $U_{alloy} = \Delta E_c$

		$N_D^+ = 10^{16}$ cm^{-3}	$N_D^+ = 10^{17}$ cm^{-3}	$N_D^+ = 10^{18}$ cm^{-3}
InN		3060	2284	1252
$In_{0.8}Ga_{0.2}N$	$U_{alloy} = \Delta E_c$	1146	973	701
	$U_{alloy} = 0$	2974	2185	1202
$In_{0.5}Ga_{0.5}N$	$U_{alloy} = \Delta E_c$	713	624	454
	$U_{alloy} = 0$	2516	1787	954
$In_{0.2}Ga_{0.8}N$	$U_{alloy} = \Delta E_c$	648	538	399
	$U_{alloy} = 0$	1803	1317	697
GaN		1371	990	544
$Al_{0.2}Ga_{0.8}N$	$U_{alloy} = \Delta E_c$	243	223	180
	$U_{alloy} = 0$	1347	978	525
$Al_{0.5}Ga_{0.5}N$	$U_{alloy} = \Delta E_c$	140	130	110
	$U_{alloy} = 0$	1139	856	454
$Al_{0.8}Ga_{0.2}N$	$U_{alloy} = \Delta E_c$	141	128	110
	$U_{alloy} = 0$	839	658	366
AlN		657	533	313

conditions of no alloy scattering and alloy scattering based on the affinity differences. In order to calibrate our calculations it is useful to begin with a comparison to previous theoretical and experimental studies. Other Monte Carlo studies [53], [54] predict an electron mobility in bulk GaN as high as 900 cm^2/Vs at 1.0×10^{17} cm^{-3} and 300 K. Our calculation for the mobility in GaN at the same doping concentration and temperature yields $\sim$990 cm^2/Vs, in reasonable agreement. A mobility greater than 800 cm^2/Vs has been reported experimentally at this doping concentration and temperature in GaN [55]. At higher doping concentrations, 9×10^{18} cm^{-3}, our model predicts a mobility of about 440 cm^2/Vs in comparison to experimental measurement of $\sim$300 cm^2/Vs [56]. Most experimental measurements apply more to a heterostructure system wherein parallel transport issues are important thus complicating comparison to bulk studies [24]. Additionally, most experimental studies are of the Hall mobility rather than the drift mobility. Direct comparison of drift mobility calculations to Hall measurements is frustrated by the high variability of the Hall factor, which is a function of the dislocation density [20]. Therefore, since dislocations are not included in the present calculations, nor known in the experimental measurements, it is difficult to provide close comparison. To the authors' knowledge no experimental mobility data exist for the ternary compounds, for AlN, and for low doped InN. The present calculations differ somewhat from our earlier full band Monte Carlo results [25]. Some of the difference is attributable to the fact that the present calculations are made using optimized band structures [37], which were not available earlier. The scattering rates are also somewhat different between the two models. In the full band simulation, the scattering rate is treated numerically at energies greater than 0.9 eV, while in the present, analytical calculations, the scattering rates are analytical for all energy ranges. It is expected that these differences in band structure and scattering rates account for the differences in the calculated velocities.

TABLE III
CALCULATED LOW FIELD MOBILITY FOR IONIZED IMPURITY CONCENTRATION OF 10^{17} cm^{-3}, AND A SET OF LATTICE TEMPERATURE OF 300 K, 450 K and 600 K. U_{alloy} STANDS FOR THE RANDOM ALLOY POTENTIAL. ΔE_c IS THE BAND GAP OFFSET. FOR $Al_xGa_{1-x}N$, AND $In_xGa_{1-x}N$ MOBILITY HAS BEEN CALCULATED FOR THE TWO BRACKETING CONDITIONS OF $U_{alloy} = 0$, AND $U_{alloy} = \Delta E_c$

		T = 300 K	T = 450 K	T = 600 K
InN		2284	1022	632
$In_{0.8}Ga_{0.2}N$	$U_{alloy} = \Delta E_c$	973	589	405
	$U_{alloy} = 0$	2185	963	594
$In_{0.5}Ga_{0.5}N$	$U_{alloy} = \Delta E_c$	624	399	273
	$U_{alloy} = 0$	1787	784	456
$In_{0.2}Ga_{0.8}N$	$U_{alloy} = \Delta E_c$	538	320	212
	$U_{alloy} = 0$	1317	537	305
GaN		990	391	215
$Al_{0.2}Ga_{0.8}N$	$U_{alloy} = \Delta E_c$	223	149	107
	$U_{alloy} = 0$	978	390	211
$Al_{0.5}Ga_{0.5}N$	$U_{alloy} = \Delta E_c$	130	93	73
	$U_{alloy} = 0$	856	332	183
$Al_{0.8}Ga_{0.2}N$	$U_{alloy} = \Delta E_c$	128	91	68
	$U_{alloy} = 0$	658	266	141
AlN		533	219	119

Table II lists the calculated low field mobilities for the binary and ternary compounds at a lattice temperature of 300 K, and a set of ionized impurity concentrations of 10^{16} cm^{-3}, 10^{17} cm^{-3}, and 10^{18} cm^{-3}. As expected, as the impurity concentration increases, the mobility decreases monotonically. In addition, the mobility decreases monotonically from InN to GaN, and from GaN to AlN in the absence of alloy scattering. However, when alloy scattering is included, the minimum mobility can be at the intermediate ternary composition, where alloy scattering is at its maximum.

Table III lists the calculated low field mobilities determined with ionized impurity concentrations of 10^{17} cm^{-3}, and a set of lattice temperatures of 300 K, 450 K, and 600 K. For comparison, the mobilities corresponding to a lattice temperature of 300 K and an ionized impurity concentration of 10^{17} cm^{-3} have been repeated from Table II. As can be seen from the table, the mobility decreases monotonically with increasing temperature due to the enhanced scattering rate. Again it is observed that for $Al_xGa_{1-x}N$ and $In_xGa_{1-x}N$, that the inclusion of alloy scattering can potentially have a major effect on the low field mobility for the temperature range studied here. It is useful to formulate an expression for the mobility of the ternary compounds that can be used for device simulation. The general expression for the low field mobility that is typically used in drift-diffusion simulations is given as

$$\mu_0(T, N) = \mu_{\min}\left(\frac{T}{300}\right)^{\beta_1} + \frac{(\mu_{\max} - \mu_{\min})\left(\frac{T}{300}\right)^{\beta_2}}{1 + \left[\frac{N}{N_{ref}\left(\frac{T}{300}\right)^{\beta_3}}\right]^{\alpha(T/300)^{\beta_4}}}. \quad (2)$$

TABLE IV
EXTRACTED PARAMETERS FOR THE LOW FIELD MOBILITY MODEL IN EQ. (2). THE REFERENCE DENSITY, N_{ref}, IS 10^{17} cm^{-3}

		μ_{min} (cm^2/V.s)	μ_{max} (cm^2/V.s)	α	β_1	β_2	β_3	β_4
InN		774	3138.4	0.68	-6.39	-1.81	8.05	-0.94
$In_{0.8}Ga_{0.2}N$	$U_{alloy} = \Delta E_c$	644.3	1252.7	0.82	-1.81	-1.30	4.84	-0.41
	$U_{alloy} = 0$	646.5	3188.7	0.66	-0.73	-3.35	2.67	0.25
$In_{0.5}Ga_{0.5}N$	$U_{alloy} = \Delta E_c$	456.4	758.1	1.04	-1.16	-1.74	2.21	-0.22
	$U_{alloy} = 0$	493.8	2659.9	0.66	-9.11	-2.14	7.19	-0.76
$In_{0.2}Ga_{0.8}N$	$U_{alloy} = \Delta E_c$	386.4	684.2	1.37	-1.36	-1.95	2.12	-0.99
	$U_{alloy} = 0$	360.9	1887.6	0.69	-0.95	-3.58	3.06	0.06
GaN		295.0	1460.7	0.66	-1.02	-3.84	3.02	0.81
$Al_{0.2}Ga_{0.8}N$	$U_{alloy} = \Delta E_c$	132.0	306.1	0.29	-1.33	-1.75	6.02	1.44
	$U_{alloy} = 0$	312.1	1401.3	0.74	-6.51	-2.31	7.07	-0.86
$Al_{0.5}Ga_{0.5}N$	$U_{alloy} = \Delta E_c$	41.7	208.3	0.12	-0.60	-2.08	10.45	2.00
	$U_{alloy} = 0$	299.4	1215.4	0.80	-5.70	-2.29	7.57	-1.08
$Al_{0.8}Ga_{0.2}N$	$U_{alloy} = \Delta E_c$	47.8	199.6	0.17	-0.74	-2.04	20.65	0.01
	$U_{alloy} = 0$	321.7	881.1	1.01	-1.60	-3.69	3.31	0.44
AlN		297.8	683.8	1.16	-1.82	-3.43	3.78	0.86

TABLE V
PARAMETERS FOR THE PROPOSED HIGH FIELD MOBILITY MODEL IN (3)

		v^{sat} (10^7 cm/s)	E_c (kV/cm)	n_1	n_2	a
InN		1.3595	52.4242	3.8501	0.6078	2.2623
$In_{0.8}Ga_{0.2}N$	$U_{alloy} = \Delta E_c$	0.8714	103.4550	4.2379	1.1227	3.0295
	$U_{alloy} = 0$	1.4812	63.4305	4.1330	0.6725	2.7321
$In_{0.5}Ga_{0.5}N$	$U_{alloy} = \Delta E_c$	0.7973	148.9098	4.0635	1.0849	3.0052
	$U_{alloy} = 0$	1.6652	93.8151	4.8807	0.7395	3.7387
$In_{0.2}Ga_{0.8}N$	$U_{alloy} = \Delta E_c$	1.0428	207.5922	4.7193	1.0239	3.6204
	$U_{alloy} = 0$	1.8169	151.8870	6.0373	0.7670	5.1797
GaN		1.9064	220.8936	7.2044	0.7857	6.1973
$Al_{0.2}Ga_{0.8}N$	$U_{alloy} = \Delta E_c$	1.1219	365.5529	5.3193	1.0396	3.2332
	$U_{alloy} = 0$	2.0270	245.5794	7.8138	0.7897	6.9502
$Al_{0.5}Ga_{0.5}N$	$U_{alloy} = \Delta E_c$	1.1459	455.4437	5.0264	1.0016	2.6055
	$U_{alloy} = 0$	2.1505	304.5541	9.4438	0.8080	8.0022
$Al_{0.8}Ga_{0.2}N$	$U_{alloy} = \Delta E_c$	1.5804	428.1290	7.8166	1.0196	2.4359
	$U_{alloy} = 0$	2.1581	386.2440	12.5795	0.8324	8.6037
AlN		2.1670	447.0339	17.3681	0.8554	8.7253

In (2), T is the temperature, N is the total doping density, and α, β_1, β_2, β_3, β_4, $\mu_{\min}$, $\mu_{\max}$, N_{ref} are parameters that can be determined either from experiment or from Monte Carlo simulation. In this case, we have used the Monte Carlo simulation to determine these parameters. We have extracted these parameters by a least squares fit of (2), to mobility data obtained from our Monte Carlo calculations. The extracted parameters for the representative compositions of the ternary compounds are shown in Table IV.

No preexisting mobility model provides a satisfactory description of the field dependence of the Monte Carlo calculated GaN mobility. Therefore, a new field dependent mobility model has been developed which is given by

$$\mu = \frac{\mu_0(T, N) + v^{sat}\dfrac{E^{n1-1}}{E_c^{n_1}}}{1 + a\left(\dfrac{E}{E_c}\right)^{n_2} + \left(\dfrac{E}{E_c}\right)^{n_1}} \quad (3)$$

where μ_0 is the low field mobility as expressed in (2). There are five parameters in the new model, which are determined from a least squares fit to the results of our Monte Carlo simulation. These parameters are v^{sat}, E_c, a, n_1, and n_2. The values of

these parameters, extracted for both ternary compounds for the two bracketing cases of alloy scattering, are shown in Table V.

IV. Conclusions

We have presented a comprehensive study of the low field electron transport dynamics in the III-nitride ternary compounds, $Al_xGa_{1-x}N$ and $In_xGa_{1-x}N$. The calculations are made using a nonparabolic effective mass band model, ensemble Monte Carlo simulation. The band parameters used in the calculation are extracted from a pseudopotential band structure calculation optimized to yield excellent agreement with experimental data and ab initio band structure models. The Monte Carlo model includes all of the important scattering mechanisms. Owing to the fact that there is no generally accepted theory of alloy scattering, we bracket its effects on the calculations by considering two extreme cases. The maximum and minimum influence of alloy scattering is examined by studying the transport without alloy scattering and with alloy scattering using the largest predicted value of the random alloy potential. Making worst case assumptions, it is found that alloy scattering can become dominant.

Calculations of the steady-state velocity field curves are presented for the binary and some representative compositions of the III-nitride ternary compounds, $In_xGa_{1-x}N$ and $Al_xGa_{1-x}N$. The inclusion of alloy scattering greatly influences the transport dynamics greatly changing the peak velocity and threshold electric field. We have further provided calculations of the low field mobility for the binary and ternary compounds. Using these calculations, we have derived a formula for the low field mobility that reflects the influence of temperature and ionized impurity concentration. In addition, we have also provided a field dependent model of the carrier mobility including parameters for the ternary compounds. Excellent agreement between the model and the Monte Carlo calculations has been obtained. The field dependent mobility model provides a highly useful and accurate description of the electron mobility in the III-nitride ternary compounds that can be incorporated into semiconductor device simulators.

Finally, it should be mentioned that the paucity of experimental data renders it presently impossible to fully calibrate our calculations. In addition, most of the experimental data for the electron mobility is determined through Hall measurements making direct comparison of the drift mobility difficult. Nevertheless, where possible we have provided comparison of our model to other calculations and experiments indicating good agreement. In addition, some clear trends have been identified that suggest interesting experiments. The effect of alloy scattering on the transport predicted by the model is obvious. The calculations predict that if alloy scattering is weak, a monotonic progression in the velocity field curves from one binary to the other occurs. However, if the alloy scattering is strong, the ternary compounds all exhibit peak velocities below that of the constituent binaries. Similar behavior occurs for the mobility.

References

[1] S. N. Mohammad, A. A. Salvador, and H. Morkoc, "Emerging gallium nitride based devices," *Proc. IEEE*, vol. 83, pp. 1306–1355, Oct. 1995.

[2] S. J. Pearton, J. C. Zolper, R. J. Shul, and F. Ren, "GaN: Processing, defects and devices," *J. Appl. Phys.*, vol. 86, pp. 1–78, July 1999.

[3] L. F. Eastman, "Results, potentials and challenges of high power GaN-based transistors," *Phys. Stat. Sol. (a)*, vol. 176, pp. 175–178, 1999.

[4] S. Nakamura, "Present status of InGaN-based laser diodes," *Phys. Stat. Sol. (a)*, vol. 176, pp. 15–22, 1999.

[5] M. S. Shur, "GaN based transistors for high power applications," *Solid-State Electron.*, vol. 42, pp. 2131–2138, 1998.

[6] K. Shenai, R. S. Scott, and B. J. Baliga, "Optimum semiconductors for high-power electronics," *IEEE Trans. Electron Devices*, vol. 36, pp. 1811–1823, Sept. 1989.

[7] M. Razeghi and A. Rogalski, "Semiconductor ultraviolet detectors," *J. Appl. Phys.*, vol. 79, pp. 7433–7473, May 15, 1996.

[8] M. Bhatnagar and B. J. Baliga, "Comparison of 6 H-SiC, 3 C-SiC and Si for power devices," *IEEE Trans. Electron Devices*, vol. 40, pp. 645–655, Mar. 1993.

[9] P. G. Neudeck, "Progress in silicon carbide semiconductor electronics technology," *J. Electron. Mat.*, vol. 24, pp. 283–288, 1995.

[10] S. Strite and H. Morkoc, "GaN, AlN, and InN: A review," *J. Vac. Sci. Tech. B*, vol. 10, pp. 1237–1266, July/Aug. 1992.

[11] E. A. Caridi, T. Y. Chang, K. W. Goosen, and L. F. Eastman, "Direct demonstration of a misfit strain-generated electric field in a [11] growth axis zinc-blende heterostructure," *Appl. Phys. Lett.*, vol. 56, pp. 659–661, Feb. 12, 1990.

[12] A. Bykhovski, B. L. Gelmont, and M. Shur, "The influence of the strain-induced electric field on the charge distribution in GaN-AlN-GaN structure," *J. Appl. Phys.*, vol. 74, pp. 6734–6739, Dec. 1993.

[13] T. F. Kuech, R. T. Collins, D. L. Smith, and C. Mailhoit, "Field-effect transistor structure based on strain-induced polarization charges," *J. Appl. Phys.*, vol. 67, pp. 2650–2652, Mar. 1990.

[14] P. M. Asbeck *et al.*, "Enhancement of base conductivity via the piezoelectric effect in AlGaN/GaN HBTs," *Solid-State Electron.*, vol. 44, pp. 211–219, 2000.

[15] B. Doshi, K. F. Brennan, R. Bicknell-Tassius, and F. Grunthaner, "The effect of strain-induced polarization fields on impact ionization in a multiquantum well structure," *Appl. Phys. Lett.*, vol. 73, pp. 2784–2786, Nov. 9, 1998.

[16] J. Kolnik *et al.*, "Electronic transport studies of bulk zinc blende and wurtzite phases of GaN based on an ensemble Monte Carlo calculation including a full zone band structure," *J. Appl. Phys.*, vol. 78, pp. 1033–1038, July 1995.

[17] B. Gelmont, K. Kim, and M. Shur, "Monte Carlo simulation of electron transport in gallium arsenide," *J. Appl. Phys.*, vol. 74, pp. 1818–1821, Aug. 1993.

[18] J. D. Albrecht *et al.*, "Electron transport characteristics of GaN for high temperature device modeling," *J. Appl. Phys.*, vol. 83, pp. 4777–4781, 1998.

[19] ——, "Monte Carlo calculation of electron transport properties of bulk AlN," *J. Appl. Phys.*, vol. 83, pp. 1446–1449, 1998.

[20] J. D. Albrecht, P. P. Ruden, E. Bellotti, and K. F. Brennan, "Monte Carlo simulation of Hall effect in n-type GaN," *MRS Internet J. Nitride Semicond. Res.*, vol. 4S1, no. G6.6, 1999.

[21] B. E. Foutz, S. K. O'Leary, M. S. Shur, and L. F. Eastman, "Monte Carlo simulation of electron transport in wurtzite aluminum nitride," *Solid State Commun.*, vol. 105, pp. 621–626, 1998.

[22] R. P. Joshi, "Temperature-dependent electron mobility in GaN: Effects of space charge and interface roughness scattering," *Appl. Phys. Lett.*, vol. 64, pp. 223–225, Jan. 1994.

[23] S. Krishnamurthy, M. van Schilfgaarde, A. Sher, and A.-B. Chen, "Bandstructure effect on high-field transport in GaN and GaAlN," *Appl. Phys. Lett.*, vol. 71, pp. 1999–2001, Oct. 1997.

[24] S. Dhar and S. Ghosh, "Low field electron mobility in GaN," *J. Appl. Phys.*, vol. 86, pp. 2668–2676, Sept. 1999.

[25] E. Bellotti *et al.*, "Ensemble Monte Carlo study of electron transport in wurtzite InN," *J. Appl. Phys.*, vol. 85, pp. 916–923, Jan. 1999.

[26] N. Mansour, K. W. Kim, and M. A. Littlejohn, "Theoretical study of electron transport in gallium nitride," *J. Appl. Phys.*, vol. 77, pp. 2834–2836, Mar. 1995.

[27] S. K. O'Leary *et al.*, "Electron transport in wurtzite indium nitride," *J. Appl. Phys.*, vol. 83, pp. 826–829, Jan. 15, 1998.

[28] T. L. Tansley and C. P. Foley, "Electron mobility in indium nitride," *Electron. Lett.*, vol. 20, pp. 1066–1068, Dec. 1984.

[29] D. L. Rode and D. K. Gaskill, "Electron Hall mobility of n-GaN," *Appl. Phys. Lett.*, vol. 66, pp. 1972–1973, Apr. 1995.

[30] W. Geertz *et al.*, "Electrical transport in p-GaN, n-InN, and n-InGaN," *Solid-State Electron.*, vol. 39, pp. 1289–1294, Sept. 1996.

[31] Z.-F. Li *et al.*, "Carrier concentration and mobility in GaN epilayers on sapphire substrate studied by infrared reflection spectroscopy," *J. Appl. Phys.*, vol. 86, pp. 2691–2695, Sept. 1999.
[32] D. P. Feng, Y. Zhao, and G. Y. Zhang, "Anisotropy in electron mobility and microstructure of GaN grown by metalorganic vapor phase epitaxy," *Phys. Stat. Sol. (a)*, vol. 176, pp. 1003–1008, 1999.
[33] M. A. Khan *et al.*, "Temperature activated conductance in GaN/AlGaN heterostructure field effect transistors operating at temperatures up to 300 C," *Appl. Phys. Lett.*, vol. 66, pp. 1083–1085, Feb. 1995.
[34] M. Farahmand and K. F. Brennan, "Full band Monte Carlo simulation of zincblende GaN MESFET's including realistic impact ionization rates," *IEEE Trans. Electron Devices*, vol. 46, pp. 1319–1325, July 1999.
[35] ——, "Comparison between wurtzite phase and zinc blende phase GaN MESFET's using a full band Monte Carlo simulation," *IEEE Trans. Electron Devices*, vol. 47, pp. 493–497, Mar. 2000.
[36] B. K. Ridley, "The low-field electron mobility in bulk AlGaN," *Phys. Stat. Sol. (a)*, vol. 176, pp. 359–362, 1999.
[37] M. Goano *et al.*, "Band structure nonlocal pseudopotential calculation of the III-nitride wurtzite phase material system—Part I: Binary compounds GaN, AlN, and InN,," *J. Appl. Phys.*, vol. 88, pp. 6467–6475, Feb. 2000.
[38] ——, "Band structure nonlocal pseudopotential calculation of the III-nitride wurtzite phase material system—Part II: Ternary alloys $Al_xGa_{1-x}N$, $In_xGa_{1-x}N$, and $In_xAl_{1-x}N$," *J. Appl. Phys.*, vol. 88, pp. 6476–6482, Feb. 2000.
[39] J. R. Hauser, M. A. Littlejohn, and T. H. Glisson, "Velocity-field relationship of InAs–InP alloys including the effects of alloy scattering," *Appl. Phys. Lett.*, vol. 28, pp. 458–461, 1976.
[40] T. Deguchi *et al.*, "Structural and vibrational properties of GaN," *J. Appl. Phys.*, vol. 86, pp. 1860–1866, 1999.
[41] V. Y. Davydov *et al.*, "Phonons in hexagonal InN: Experiment and theory," *Phys. Stat. Sol. (b)*, vol. 216, pp. 779–783, 1999.
[42] V. Y. Davydov *et al.*, "Phonon spectrum of wurtzite GaN and AlN. Experiment and theory," *J. Cryst. Growth*, vol. 189/190, pp. 656–660, 1998.
[43] K. Karch, J.-M. Wagner, and F. Bechstedt, "Ab initio study of structural, dielectric, and dynamical properties of GaN," *Phys. Rev. B*, vol. 57, pp. 7043–7049, 1998.
[44] K. Karch and F. Bechstedt, "Ab initio lattice dynamics of BN and AlN: Covalent versus ionic forces," *Phys. Rev. B*, vol. 56, pp. 7404–7415, 1997.
[45] V. W. L. Chin, T. L. Tansley, and T. Osotchan, "Electron mobilities in gallium, indium, and aluminum nitrides," *J. Appl. Phys.*, vol. 75, pp. 7365–7372, 1994.
[46] K. Shimada, T. Sota, and K. Suzuki, "First-principles study on electronic and elastic properties of BN, AlN, GaN," *J. Appl. Phys.*, vol. 84, pp. 4951–4958, 1998.
[47] B. E. Foutz, S. K. O'Leary, M. S. Shur, and L. E. Eastman, "Transient electron transport in wurtzite GaN, InN, and AlN," *J. Appl. Phys.*, vol. 85, pp. 7727–7734, 1999.
[48] M. A. Littlejohn *et al.*, "Alloy scattering and high field transport in ternary and quaternary III-V semiconductors (FET model)," *Solid-State Electron.*, vol. 21, pp. 107–114, Jan. 1978.
[49] V. W. L. Chin, B. Zhou, T. L. Tansley, and X. Li, "Alloy-scattering dependence of electron mobility in the ternary gallium, indium, and aluminum nitrides," *J. Appl. Phys.*, vol. 77, pp. 6064–6066, 1995.
[50] J. C. Phillips, "Ionicity of the chemical bond in crystals," *Rev. Mod. Phys.*, vol. 42, pp. 317–354, 1970.
[51] J. D. Albrecht *et al.*, "Monte Carlo calculation of high- and low-field $Al_xGa_{1-x}N$ electron transport characteristics," *Proc. Nitride Semiconductors Symp.*, pp. 15–20, 1998.
[52] S.-H. Wei and A. Zunger, "Valence band splittings and band offsets of AlN, GaN, and InN," *Appl. Phys. Lett.*, vol. 69, pp. 2719–2721, Oct. 1996.
[53] U. V. Bhapkar and M. Shur, "Monte Carlo calculation of velocity-field characteristics of wurtzite GaN," *J. Appl. Phys.*, vol. 82, p. 1649, 1997.
[54] B. E. Foutz, I. F. Eastman, U. V. Bhapkar, and M. A. Shur, "Comparison of high field electron transport in GaN and GaAs," *Appl. Phys. Lett.*, vol. 70, p. 2849, 1997.
[55] D. C. Look *et al.*, "Defect donor and acceptor in GaN," *Phys. Rev. Lett.* , vol. 79, p. 2273, 1997.
[56] D. Feiler *et al.*, "Pulsed laser deposition of epitaxial AlN, GaN, and InN thin films on sapphire (0001)," *J. Cryst. Growth*, vol. 171, pp. 12–20, Jan. 1997.

Maziar Farahmand (M'95) received the B.S. and M.S. degrees in electronics from the Sharif University of Technology, Iran, in 1992 and 1994, respectively, and the Ph.D. degree in 2000 from Georgia Institute of Technology, Atlanta.

From 1994 to 1996, he was a Faculty Member at Razi University, Iran, and then joined the Physical Electronics Research Group, Chalmers University, Sweden. In 1996, he joined the Computational Electronics Research Group. He is currently with Movaz Networks, Norcross, GA.

Carlo Garetto received the Laurea degree in electronics engineering from Politecnico di Torino, Torino, Italy in 2000.

From June to December, 2000, he was with the Department of Information Technology, Mid-Sweden University, Sundsvall, Sweden. He is currently engaged in research on the electrical and transport properties of wide bandgap semiconductors.

Enrico Bellotti was born in Italy in 1963. He received the "Laurea in Ingegneria Elettronica" degree from the Politecnico di Milano, in 1989, and the Ph.D. degree in 1999 from the Georgia Institute of Technology, Atlanta, GA.

During 1990, he was with the Italian Army for mandatory military service. From 1991 to 1993, he was with Schlumberger Industries, Italy. In 1994 he joined AMRT, Advanced Meter Reading Technology, a joint venture partnership between Schlumberger Industries and Motorola, Inc. Norcross, GA. From June 1999 until August 2000, he was a Research Engineer with the Computational Electronics Group, Georgia Institute of Technology. Since then, he has become an Assistant Professor of Electrical Engineering at Boston University, Boston, MA. His research interests are in the area of semiconductor electronic structure calculation, physics and transport properties of wide bandgap semiconductors, and computational electronics.

Kevin F. Brennan (SM'90) received the B.S. degree in physics from the Massachusetts Institute of Technology, Cambridge, and the M.S. degree in physics and Ph.D. degree in electrical engineering from the University of Illinois at Urbana-Champaign.

He is a Professor of electrical and computer engineering at the Georgia Institute of Technology, Atlanta, GA, where he has been since 1984. His research interests lie in the general area of semiconductors and microelectronics, with a particular emphasis on the physics and device application of emerging semiconductor materials for future high-power, high-frequency and photonic detection applications. His research experience includes the design, evaluation and optimization of infrared, optical and ultraviolet photonic detectors and emitters. He has published numerous papers in scientific peer reviewed journals, has five U.S. patents, and is the author of *The Physics of Semiconductors with Applications to Optoelectronic Devices* (Cambridge, U.K.: Cambridge University Press, 1999).

Michele Goano (M'98) received the Laurea and Ph.D. degrees in electronics engineering from Politecnico di Torino, Torino, Italy in 1989 and 1993, respectively.

In 1994 and 1995, he was a Postoctoral Fellow in the Departement de Genie Physique, Ecole Polytechnique de Montreal, Montreal, QC, Canada. Since 1996, he has been a Research Assistant in the Dipartimento di Elettronica, Politecnico di Torino. From September 1998 to February 1999, and from November 1999 to February 2000, he was a Visiting Scholar at the School of Electrical and Computer Engineering, Georgia Institute of Technology, Atlanta. From November 2000 to January 2001, he was a Visiting Scholar at the the Department of Electrical and Computer Engineering, Boston University, Boston, MA. He has been engaged in modeling of semiconductor optical components and Monte Carlo simulation of quantum-well devices, and is currently involved in research on coplanar components, traveling wave modulators, and wide bandgap semiconductors.

Enrico Ghillino received the Laurea degree in electronics engineering from Politecnico di Torino, Torino, Italy in 2000.

From June to December, 2000, he was at the Department of Information Technology, Mid-Sweden University, Sundsvall, Sweden. He is currently engaged in research on the electrical and transport properties of wide bandgap semiconductors.

Giovanni Ghione (SM'94) graduated in electronics engineering from Politecnico di Torino, Torino, Italy in 1981.

From 1983 to 1987, he was a Research Assistant with Politecnico di Torino. From 1987 to 1990, he was an Associate Professor with Politecnico di Milano, Milano, Italy. In 1990 he joined the University of Catania, Catania, Italy as Full Professor of Electronics. Since 1991, he has been a Full Professor at II Faculty of Engineering, Politecnico di Torino. Since 1981, he has been engaged in Italian and European research projects (ESPRIT 255, COSMIC and MANPOWER) in the field of active and passive microwave CAD. His present research interests concern the physics-based simulation of active microwave and optoelectronic devices, with particular attention to noise modelling, thermal modelling, active device optimization. His research interests also include several topics in computational electromagnetics, including coplanar component analysis. He has published more than 150 papers and book chapters in the above fields.

Prof. Ghione is member of the Associazione Elettrotecnica Italiana. He is an Editorial Board member of the IEEE TRANSACTIONS ON MICROWAVE THEORY AND TECHNIQUES.

John D. Albrecht received the Ph.D. degree in electrical engineering from the University of Minnesota, Minneapolis, in 1999.

In 1999, he joined the Electronic Science and Technology Division, Naval Research Laboratory, Washington, DC, where he is currently a National Research Council Post-Doctoral Fellow. His research includes studies of carrier transport in wide bandgap semiconductors, device physics, and computational models of mesoscopic composites.

P. Paul Ruden (M'88–SM'92) received the Ph.D. degree in physics from the University of Stuttgart, Germany, in 1982.

He worked on semiconductor superlattices at the Max Planck Institute for Solid State Research in Stuttgart, West Germany, from 1979 to 1983. From 1983 to 1985, he was with the Electronics Science and Technology Division, Naval Research Laboratory, Washington, DC, and also with the Department of Electrical and Computer Engineering, North Carolina State University, Raleigh. In 1985, he joined the Corporate Research Laboratory, Honeywell Inc., Bloomington, MN, where he led research efforts in the areas of semiconductor photodetectors and III–V heterostructure field effect transistor technology. Since 1989, he has been on the faculty of the Department of Electrical and Computer Engineering, University of Minnesota, Minneapolis, where he is currently Professor of electrical engineering. His research focuses on modeling of semiconductor materials and devices. He has published over 100 papers in technical journals in these fields.

Dr. Ruden is a member of the American Physical Society and the Materials Research Society.